International Journal of Mechanical Engineering and Technology (IJMET)
Volume 8, Issue 7, July 2017, pp. 256–266, Article ID: IJMET_08_07_030
Available online at http://www.iaeme.com/IJMET/issues.asp?JType=IJMET&VType=8&IType=7
ISSN Print: 0976-6340 and ISSN Online: 0976-6359

NULL STRESS PLANES GRAPHS THROUGH NUMERICAL SIMULATIONS OF A BEAM SUBJECTED TO VARIABLE BENDING STRESS

R.A. González-Lezcano
Department of Architecture and Design, Escuela Politécnica Superior,
Universidad CEU San Pablo, Boadilla del Monte, Madrid, Spain

R. Guzmán-López
Facultad de Ingeniería Mecánica, Universidad Pontificia Bolivariana,
Campus Universitario Autopista Piedecuesta Km. 7, Bucaramanga-Colombia

ABSTRACT

In engineering, how solid materials behave to environment and external forces (such as tensile and compressive forces, torsion, bending and shear) must be known. The threats to structural elements can be categorized in time factor and failure models, such as: time-dependent, time-independent, stable over time. Time-dependent threats (Stress Corrosion Cracking (SCC), corrosion and plastic deformation) and time-independent threats (natural forces, damage caused by third parties, improper operations) are random events and their appearance is generally not predictable. Stable over time threats, such as both construction and manufacturing defects are possibly considered as time-dependent due to its potential growth generated by load cycles. However, potential failure of any defect can be increased by the effects of fatigue induced by load cycles. This paper shows how the magnesium alloy ZC71 reinforced with silicon carbide (SiC), when subjected to cyclic loading, can have two or three null stress zones which can lead to variations in the equilibrium equations of the Strength of Materials. Different tension and compression behaviors can accentuate the appearance of these areas in such a way that they are not necessarily symmetrical to a neutral axis, in the case of bending, which can result in not as predictable fracture behavior over time. Numerical simulations have been made of a homogeneous beam of rectangular section where alternating loads which are capable of plasticize the material have been applied. The material has different behavior in both tension and compression as it plasticizes in some compressive load magnitudes or in tensile and compressive load magnitudes. Numerical simulations of a homogeneous material with the same behavior in both tension and compression are also performed. In every case null stress graphs in the cross section of the beam are created. In these graphs, variations of the neutral axis can be seen once the beam has plasticized and loading and unloading of loads are being made.

Key words: Material Resistance; Numerical Simulation; Fatigue; Alternating Forces; Cyclic Loads.

Cite this Article: R.A. González-Lezcano and R. Guzmán-López, Null Stress Planes Graphs Through Numerical Simulations of A Beam Subjected To Variable Bending Stress. *International Journal of Mechanical Engineering and Technology*, 8(7), 2017, pp. 256–266.
http://www.iaeme.com/IJMET/issues.asp?JType=IJMET&VType=8&IType=7

1. INTRODUCTION

When materials are subjected to fatigue, a progressive fracture appears. This fact causes permanent deformation of the different mechanical and/or structural components. In many cases, this slow deformation ceases because of the disappearance of the force which produces it, due to the deformation itself. When plastic-elastic deformation continues for a long time, the material is then broken. In this paper magnesium alloy reinforced with SiC particles, which is subjected to repeated or cyclical stress, for example a vibration, is analyzed. Although the maximum effort never exceeds the yield strength, the material can break even after a short time. In the fatigue, any apparent deformation is observed, but small cracks are developed. These cracks propagate through the material until the rest of the effective area cannot support the cyclic load maximum effort. Knowledge of the tensile stress, the yield strengths, the plastic-elastic deformation resistance of the materials and the fatigue are extremely important in engineering design.

Many of the elements of construction engineering and mechanical engineering are subjected in service to variable loads, the design of the elements subjected to variable loads should be done by a theory that takes into account the factors that influence the emergence and development of cracks, which can lead to failure after a number of repetitions (cycles) of effort. The growing interest of the designers in having materials, which combine good mechanical properties with low weight, has led to a significant development of metallic matrix composite materials. The presence of reinforcement (fiber or particle) gives these materials interesting mechanical properties.

2. METHODOLOGY

In this paper, numerical simulations of a composite material beam, of metallic matrix reinforced with ceramic particles, at room temperature (23ºC) are developed. The evolution of the neutral axis and the plastic areas are studied. The paper aims to address the following objectives:

- Characterize the ZC71 magnesium alloy reinforced with silicon carbide particles with both a tensile and compression test respectively.
- Analyze the influence of different material behavior in tension and compression in a structural element of PMMC's subjected to alternating bending loads.
- Determine the effect produced by different yield strengths (tensile and compressive) in the unloading status.
- Develop the null stress graphs in the central cross section of the beam and thus check the relationship between the plastic-elastic borders of the stress profile with the null stress points. These numerical results can be provided as a study which could incentive to material resistance theories to mathematical formulations that include the offset of the neutral axis in both loading and unloading situations when mechanical elements are plasticized.
- Compare the numerical results with analytical predictions.

2.1. Material

The mechanical properties of the reinforced magnesium alloy have been obtained through quasi static tension and compression tests. A servo-hydraulic testing machine has been used with a 0.02 s^{-1} strain rate. Figure 1 shows stress-strain curves which have been made in both tension and compression on the metallic matrix composite material ZC71 reinforced with ceramic SiC particles in 12%.

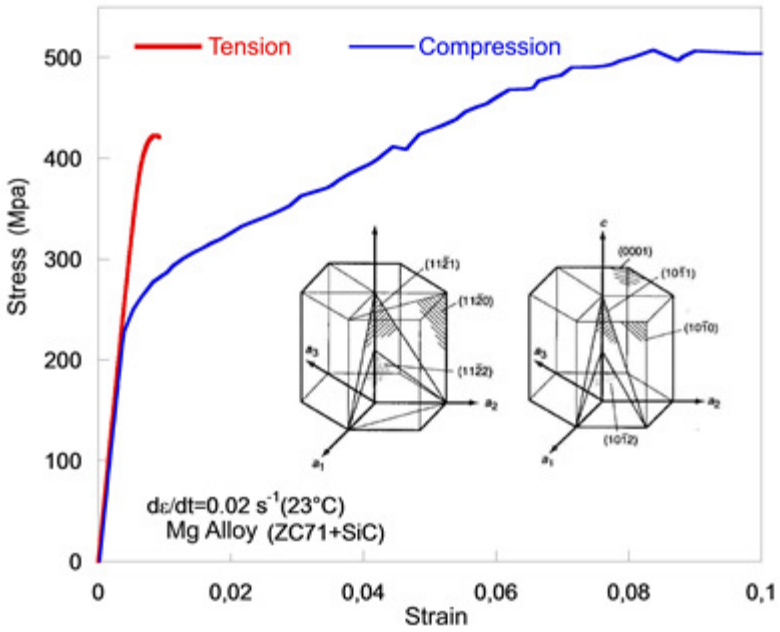

Figure 1 Stress-strain curves in tension and compression on the ZC71 magnesium alloy reinforced with SiC particles.

Magnesium forms hexagonal crystallographic compact structures (HCP). This structure is very common in metals (beryllium, titanium, zinc) and it strongly influences its behavior in σ-ε curves. At room temperature (20ºC) the only slip plane is (0001) and the corresponding slip direction is [1120] (see Figure 1); from 225ºC other slip planes appear which are (1011) and (1012). Cleavage planes are (0001), (1011), (1012) and (1010) (Schmid, 1950).

2.2. Numerical Analysis

Finite elements commercial software ABAQUS/Standard was used for simulation. The 3D model is a rectangular beam with a cross section of 0.25 m x 0.25 m and a length of 1.8 m. It is subjected to a uniformly distributed load and with a cyclic temporal variation (see Figure 2). Figure 3 shows a graph of the load constituted by three load cycles. Regarding the amplitude of the cyclic loading, three cases have been considered. In the first one (Case A) the amplitude of the applied load is 4.0 MN/m^2, in the second one (Case B) the amplitude of the applied load is 4.9 MN/m^2 and in the third case (case C) the amplitude of the load is 3.5 MN/m^2. In the study, the kinematic hypothesis known as Navier-Bernoulli hypothesis has been considered to be used, where, in the deformation of the prismatic solid, normal plane sections remain plane after deformation. Furthermore, it is assumed that the normal plane sections are non-deformable in its plane, this hypothesis allows obtaining displacements at any point of the cross section from only six degrees of freedom (rigid plane position), associated normally to the three displacement components and to the three components of the center of gravity (G) rotation of the cross section.

Cyclic loads result in unloading stresses in the material; so that if the material has residual stresses or permanent deformation upon reaching the maximum load, permanent deformation will always be present in the material although the load has disappeared altering the balance of cross section in the following uploads and downloads.

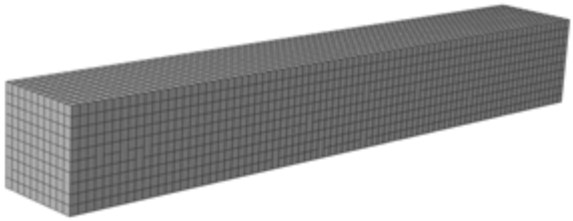

Figure 2 Mesh of the beam in the numerical model

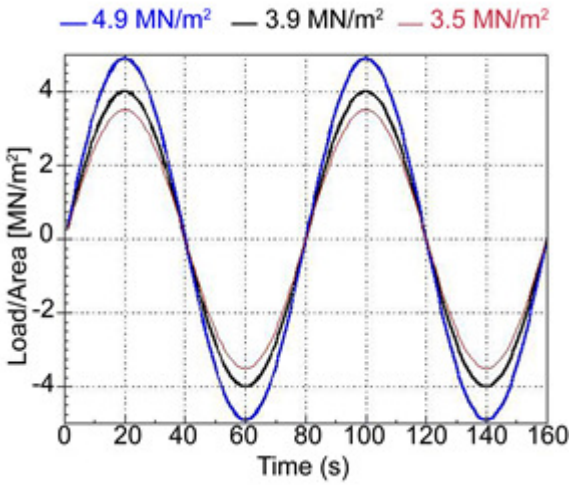

Figure 3 Cyclic load applied

3. NUMERICAL RESULTS AND DISCUSSION

The process of obtaining the profile of normal stresses to the central section of the beam for a given instant t_0 depends on its entire previous history of stresses. In each case the stresses profile is obtained by adding to the stresses profile in $t = t_0$ (s), the increased stresses caused by the load applied in the time interval corresponding to the elastic unloading.

CASE A. In the loading process, the neutral fiber will maintain a value of 0.5L while the material has not plasticized as it starts to plasticize first during compression at the top of the beam. In order to reach the equilibrium of moments in the cross section of the beam, the neutral axis will scroll below 0.5L, so that when the load has reached the maximum value in 20, the neutral axis is located in 0.6L.

Figure 4 shows the time when the load has reached the maximum value. The upper fiber has plasticized to a greater extent than the lower fiber unloading from 20s to 42.75s (as seen in the unloading). The result will be the appearance of null stress in the central cross section due to the appearance of two local maxima that match the elastic-plastic borders of the materials when it had reached the maximum load.

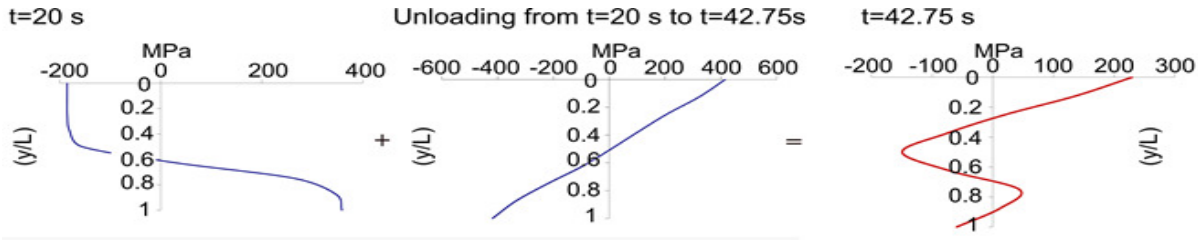

Figure 4 Stress status of the cross section for t=20s and t=42.75s

Figure 5 shows the stress-strain diagrams which have be obtained in both the lower (figure 5.a.) and upper (figure 5.b.) fibers in the time interval [0, 42.75s]. The sign change in the stress in both fibers (lower and upper) can be seen as a result of the sign change of the load.

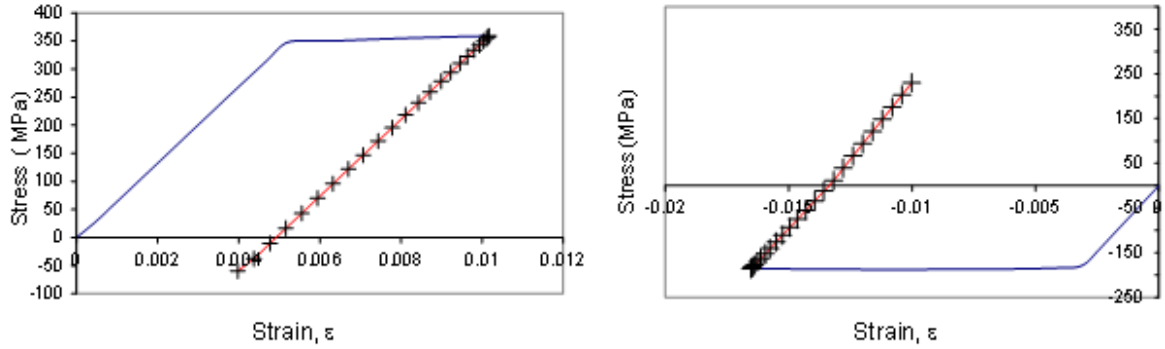

Figure 5 Stress-strain diagrams of the cross section for the time interval [0, 42.75 s] in both **a**) lower fibers and **b)** upper fibers

Figure 6 diagrams, in t=59.75 s, when the load is about the reach the maximum value in the opposite direction, it can be seen how the neutral axis reaches a value close to 0.4L moving upwards. In the unloading process up to 80 s, two null stress points appear, and just over 80 s three points appear due to the load between 80 and 100 s.

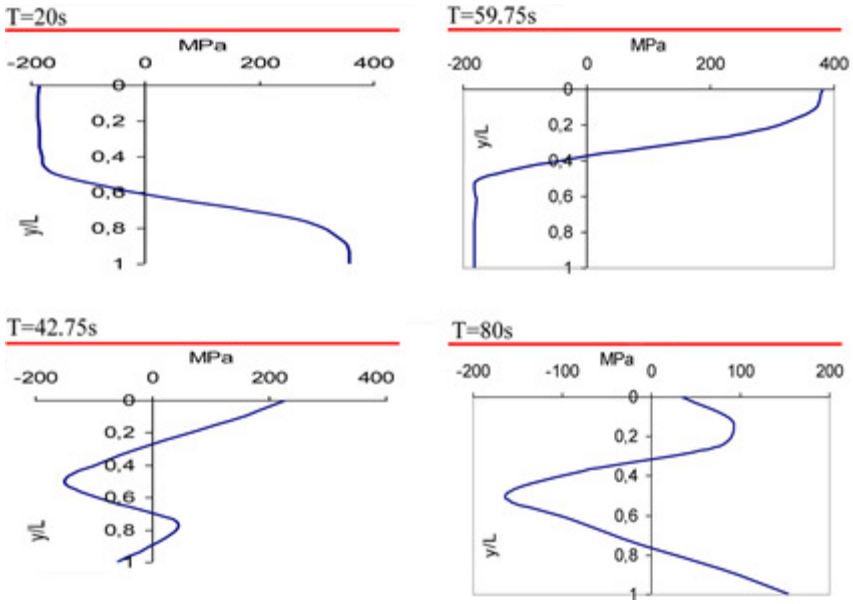

Figure 6 Stress status of the cross section for t=20 s, t=42.75 s, t=59.75 s and t=80 s

In the graphs of Figure 7, for t = 100 s, after the second loading in the positive direction, it can be seen how the fibers are a permanent deformation which causes the placement of the

neutral axis in 0.6L, and in 0.4L after the second loading in the negative direction. In the 120 s and 160 s, two points of null stress can be seen, from 120 s to 122.75 s. From 160 s to 162.75 s three points of null stress appear due to unloading that occur in both cases (loads in the opposite direction).

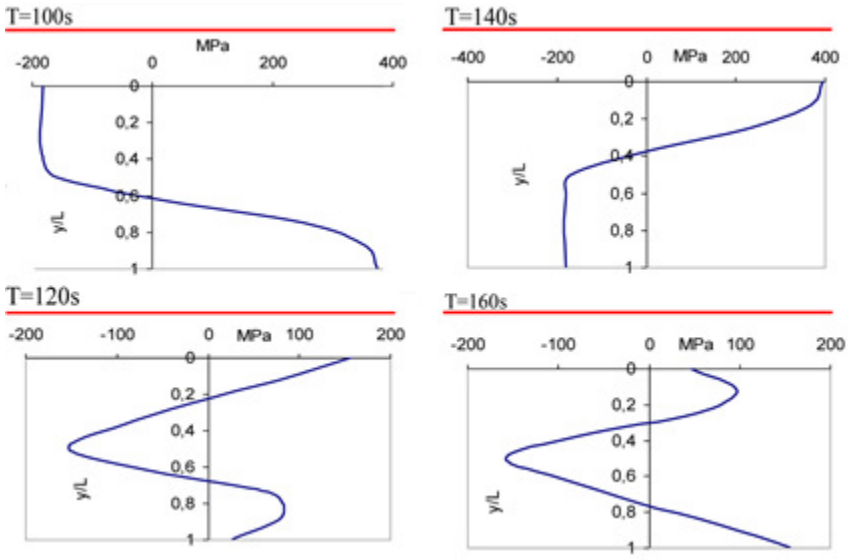

Figure 7 Stress status of the cross section for t=100 s, t=120 s, t=140 s and t=160 s

Figure 8 shows the respective stress-strain diagrams in both upper and lower fibers in the time interval [0, 160 s].

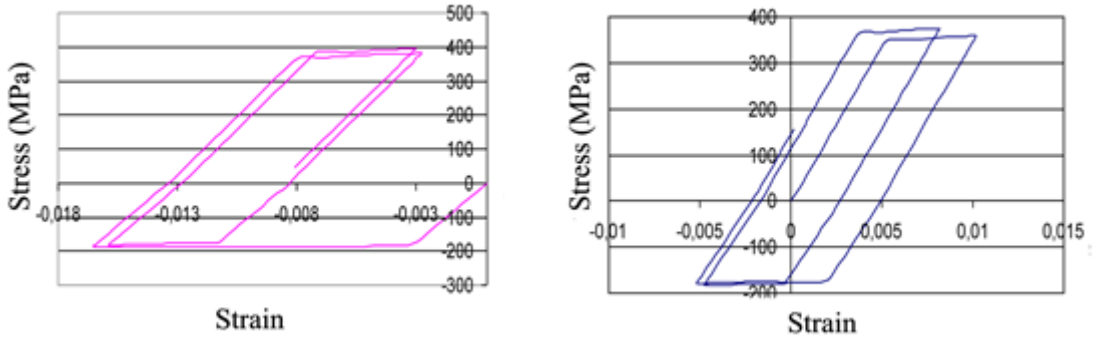

Figure 8. Stress loading and unloading in both upper and lower fibers of the central cross section of the beam in the time interval [0, 160 s].

Figure 9 shows the evolution over time of the width of the plasticized upper and lower areas. The following details can be seen:

- The section initiates its plasticizing in the upper fiber when compressing.
- At t = 20 s at maximum load, the plasticized compression area is much higher (38% of the section) that the plasticized tensile area.
- At t = 60 s the load is reversed as it passes to be under compression suffering therefore this fiber a sharp plasticizing.

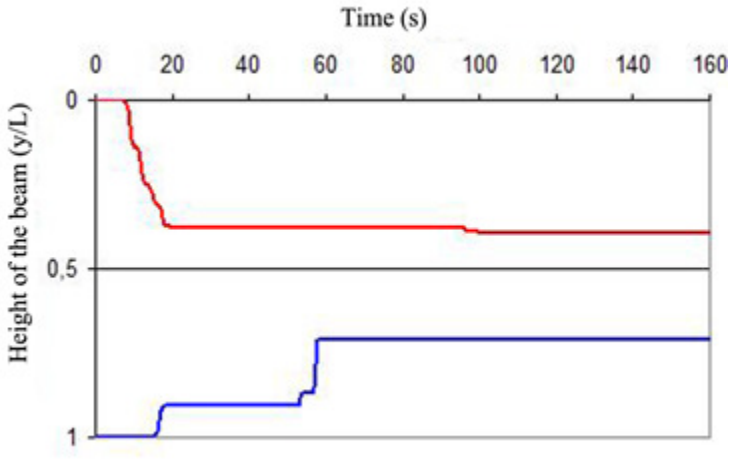

Figure 9 Evolution of the width of the plasticized area

Increasing the plasticized zone will create a section subjected to a diminishing elastic stresses, which will cause that, in repeated cycles, a sudden failure can occur. The accumulation of damage, which can be seen in figure 9, can be identified by the following expression: as plasticizing curves in cross section approach, it indicates that the cross section is about to suffer sudden breakage because the plasticized area is such that normal stresses will create breakage in the elastic cross section [18]. By reducing the part of the cross section which works in elastic rate, breakage will sudden occur in values below the yield strength [19].

CASE B. A case has been simulated where the material will only lead to plasticizing compression. The amplitude of the cyclic loading has become equal to 4.0 MN / m^2, whereby the material is initially only carried to plasticizing by compression.

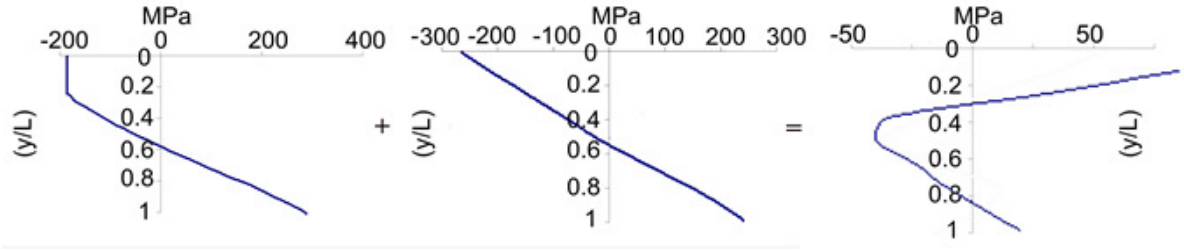

Figure 10 Stress status of the cross section for t=40 s

It can be seen that there is only elastic-plastic border in the stress profile achieved in t = 40 s which corresponds to the area under compression. When elastic unloading happens, only local border will appear, therefore, two null stress points will rise.

CASE C.- This case has been simulated to study the behavior of a material with equal tensile and compressive behavior to compare this one with cases discussed above. In this case the tensile behavior (figure 1) has been considered equal to the compression and the amplitude of the load has become equal to 3.5 MN / m^2, thus, the material is carried to the initial plasticizing in both tension situations.

3.1. Stress Planes Graphs

Stress planes graphs are presented below for the three simulated cases (A, B and C). For case A, figure 11 shows the evolution in time of the location of the neutral fiber. At the beginning of the application of the load, plasticizing occurs in the compressed area and therefore the neutral axis steps down faster to the tensile zone.

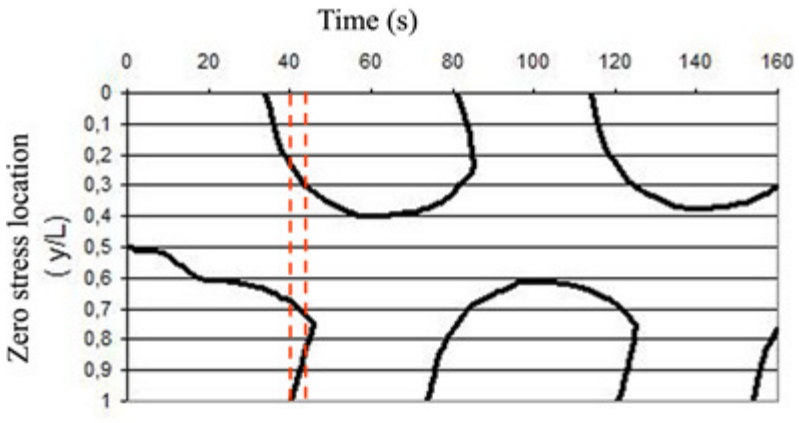

Figure 11. Evolution of the neutral fiber in case A

The graph shows the appearance, in few moments of time, of three null stress points (neutral fibers). These three neutral fibers coexist, for example, in the time interval [40.5 s, y 46.75s]. They appear at the time when the load begins to change its sign and are due to residual stresses that appear first in the compressed area (where the appearance of residual stresses can be seen at 34.5 s, approximately) and then in the tensile area. Non-simultaneous occurrence of residual stresses is that the elastic-plastic boundaries differ in the material as it does not behave similarly when being under tension or compression. It may be noted that, following the example of the interval [40.5 s, y 46.75s], two of the neutral axes coincide at one at the end of that time interval; this neutral axis is then closer to the tensile area.

Figure 12 shows the evolution in time of the location of the neutral fiber. As in the previous case, from t=10 s, plasticizing occurs in the compressed area and therefore the neutral axis steps down faster to the tensile zone. From t=20 s to t=40 s, some of the fibers under compression will be under tension but closer to the lower fiber. Fibers subjected to tension will remain the same, therefore another null stress point does not appear.

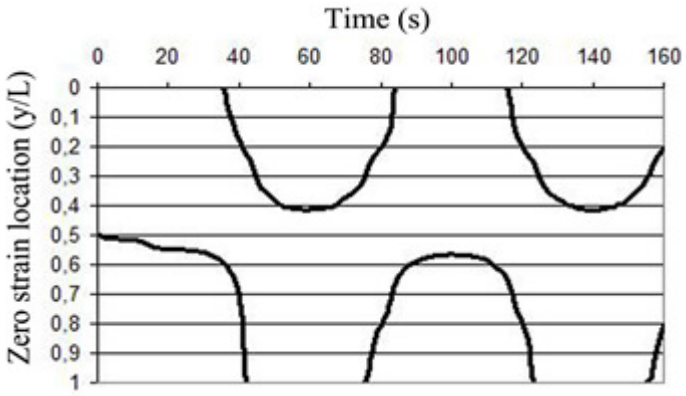

Figure 12 Evolution of the neutral fiber in case B

Figure 13 shows the evolution of the position of the neutral fiber during the application of the load (two cycles of 80 s). How the neutral line remains at the medium fiber of the section can be seen, but on reaching the vicinity of 40 s, two other null stress points located symmetrically start to appear. This is because the unloading causes a symmetrical distribution of residual stresses. The apparent loss of symmetry at t = 85 s or t = 125 s is possibly due to numerical reasons.

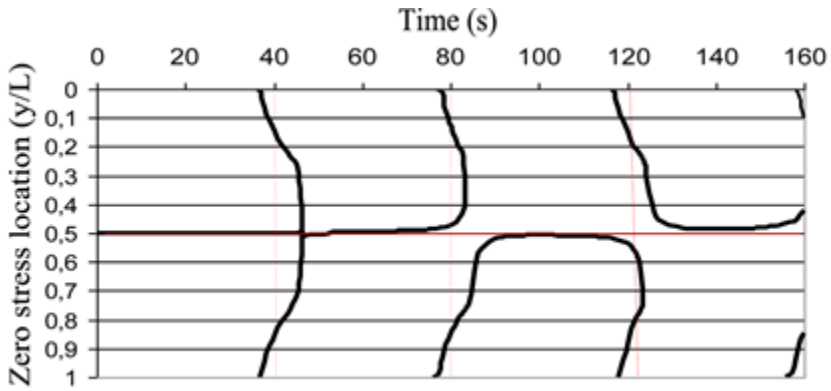

Figure 13 Evolution of the neutral fiber in case C

4. CONCLUSIONS

The difference in the behavior of the material under both tension and compression has significant influence, especially when the material is subjected to cyclic loading. In the case of a beam, the difference in this behavior results in alterations in the position and number of lines or neutral axes and in the position of the elastic-plastic boundaries. The numerical results can be predicted using general theories of Resistance of Materials.

The materials are subjected to alterations of their equilibrium condition in service; both having different tensile and compressive behavior (cast iron and in our case the metal matrix composite ZC71) as well as metals like steel, aluminum, etc. When subjected to cyclic loading, as shown in the case C, there are moments of time that permanent deformations can produce two null stress points, although in cases of equal tension and compression behavior, null stress points are symmetrical approximating the behavior to basic theories of equilibrium of the cross section of a continuous beam.

It is known that this work hardening is a material hardening because of a plastic deformation macroscopically which has the effect of increasing the dislocation density of the material deformation. As the material is saturated with new dislocations, resistance to formation of new dislocations and their movement is created. This resistance to the formation and movement of dislocations manifests macroscopically as a resistance to plastic deformation. This movement of dislocations is what produces the plastic deformation (irreversible) as propagated by the crystal structure. At normal temperatures when a material deforms, dislocations are also created (in such a way that they exceed the ones that disappear), and cause tensions in the material, preventing other dislocations the free movement of these. This leads to increased material strength and the consequent decrease in ductility and the material will fail because of fatigue in its service life; but this study helps us to try to predict which behavior may have the metal in times prior to fracture service, to try to infer more knowledge the time of the breakage.

A graph of neutral fiber helps to establish the appropriate equilibrium depending on the stress state of the cross section and to predict the behavior of the material once started plasticization, being very useful for materials that can absorb great deformation energy before breakage.

Suitable heat treatment can reduce residual stresses trapped in the plasticizing process for possible reuse of the material.

The plastic moment born in cross section under compression plus bending moment must be balanced with the plastic moment under tension plus the bending moment.

It would be necessary to establish the behavior of partially or fully laminated areas in different types of cross section to more accurately predict behavior in service of any plasticized

cross section during work cycles, if the cumulative damage of a plasticized metal without cracking zones, or breaks, can play an additional service.

ACKNOWLEDGEMENTS

The authors wish to thank Universidad CEU San Pablo (Madrid, Spain) and Universidad Pontificia Bolivariana (Bucaramanga, Colombia) for facilities and resources provided. The authors would like to express their gratitude to Carlos III de Madrid Engineering Department.

REFERENCES

[1] Dolce, M; Cardone, D. Mechanical behaviour of shape memory alloys for seismic applications 1. Martensite and austenite NiTi bars subjected to torsion. International Journal of Mechanical Sciences 2001:43(11) 2631-2656

[2] Alfredsson, Olsson, M. Standing contact fatigue. Fatigue & Fracture of Engineering Materials & Structures 1999:22(3) 225-237

[3] Baragetti, S. Fatigue resistance of steel and titanium PVD coated spur gears. International Journal of Fatigue 2007:29(911) 1893-1903

[4] Hokka, M.; Leemet, T.; Shrot, A.; Baeker, M.; Kuokkala, V. T. Characterization and numerical modeling of high strain rate mechanical behavior of Ti153 alloy for machining simulations. Materials Science and Engineering Astructural 2012:550 350-357

[5] Hallberg, Hakan; BanksSills; Ristinmaa, Matti. Crack tip transformation zones in austenitic stainless steel. Engineering Fracture Mechanics 2012:79 266-280

[6] Baragetti, S; Tordini, F. A numerical study on the fatigue and rolling contact fatigue behaviour of PVDcoated steel and titanium spur gears. Engineering with Computers 2011:27(2) 127-137

[7] Hokka, M.; Gomon, D.; Shrot, A.; Leemet, T.; Baeker, M.; Kuokkala, V. T. Dynamic Behavior and High Speed Machining of Ti6246 and Alloy 625 Superalloys: Experimental and Modeling Approaches. Experimental Mechanics. 2014:54 (2): 199-210

[8] Milesi, M; Chastel, Y; Hachem, E; Bernacki, M; Loge, RE; Bouchard, PO. A multiscale approach for high cycle anisotropic fatigue resistance: Application to forged components. Materials Science and Engineering Astructural Materials Roperties Microstructure and Processing 2010:527(1819) 4654-4663

[9] Brighenti, Roberto; Scorza, Daniela. Numerical modelling of the fracture behaviour of brittle materials reinforced with unidirectional or randomly distributed fibres. Mechanics Of Materials 2012:52 12-27

[10] Drozdov, A. D.; Christiansen, JD. Cyclic viscoelastoplasticity of polypropylene/nanoclay composites. Mechanics of Timedependent Materials 2012:16(4) 397-425

[11] Dutta, N; Rasty, J. Prediction of ElasticPlastic Boundary around ColdExpanded Holes Using Elastic Strain Measurement. Journal of Engineering Materials and Technology transactions of The ASME 2010:132(3)

[12] Gurunathan, C.; Gnanamoorthy, R.; Jayavel, S. Prediction of frictional heating and temperature distribution in selective ceramicreinforced polymer composite. Proceedings of The Institution Of Mechanical Engineers Part J-Journal Od Engineering Tribology 2014:228 (12): 1433-1442

[13] Lei, Y; Zhu, WQ. Fatigue crack growth in degrading elastic components of nonlinear structural systems under random loading. International Journal Of Solids And Structures 2000:37(4) 649-667

[14] Glodez, S; Flasker, J; Ren, Z. A new model for the numerical determination of fitting resistance of gear teeth flanks. Fatigue & Fracture Of Engineering Materials & Structures 1997:20(1) 71-83

[15] Le Pecheur; Curtit, F; Clavel, M; Stephan, JM; Rey, C; Bompard, P. Polycrystal modelling of fatigue: Prehardening and surface roughness effects on damage nitiation for 304L stainless steel. International Journal of Fatigue 2012:45: 48-60

[16] Correa, C; Ruiz de lara, L.; Diaz, M.; Porro, J. A.; GarciaBeltran,; Ocana, J. L. Influence of pulse sequence and edge material effect on fatigue life of Al2024T351 specimens treated by laser shock processing. International Journal of Fatigue 2015; 70: 196-204.

[17] Lei, Y; A stochastic approach to fatigue crack growth in elastic structural components under random loading. Acta Mechanica 1999:132(14) 63-74

[18] Bolotin, VV; Belousov, IL. Early fatigue crack growth as the damage accumulation process. Probabilistic Engineering Mechanics 2001:16(4) 279-287

[19] Fajdiga, G; Glodez, S; Kramar, J. Pitting formation due to surface and subsurface initiated fatigue crack growth in contacting mechanical elements. WEAR 2007:262(910) 1217-1224

[20] Smoljan, B; Iljkic, D; Traven, F. Predictions of Mechanical Properties of Quenched and Tempered Steel. Strojniski Vestnikjournal of Mechanical Engineering 2010:56(2) 115-120

[21] Majzoobi, GH; Motlagh, ST; Amiri, A. Numerical simulation of residual stress induced by rollpeening. Transactions of The Indian Institute Of Metals 2010:63(23) 499-504.

[22] Dr J M Prajapati and P A Vaghela, Factor Affecting The Bending Stress at Critical Section of Asymmetric SPUR Gear, 4(4), July - August (2013), pp. 266-273, *International Journal of Mechanical Engineering and Technology*.

[23] Kalpana Mohan and S. P. Vijaykumar, Analysis of Bridge Girder with Beam and without Beam. International Journal of Civil Engineering and Technology, 7(5), 2016, pp.337–346

[24] Aparna C Manoharan and R.K. Tripathi, Analysis of Steel Beams with Single Opening at Different Locations. International Journal of Civil Engineering and Technology, 8(5), 2017, pp. 539–551.

[25] Jalalahmadi, B; Sadeghi, F; Peroulis, D. A Numerical Fatigue Damage Model for Life Scatter of MEMS Devices. Journal of Microelectro mechanical Systems 2009:18(5) 1016-1031

[26] Glodez, S; Winter, H; Stuwe, HP. A fracture mechanics model for the wear of gear flanks by pitting. WEAR 1997:208(129 177-183